



# A Review of Thermally Sprayed Polymer Coatings

Heli Koivuluoto<sup>1</sup>

Submitted: 3 November 2021 / in revised form: 10 April 2022 / Accepted: 11 April 2022 / Published online: 12 May 2022  
© The Author(s) 2022

**Abstract** Thermal spraying of polymer coatings has been applied for many decades. Initially, the focus was primarily on corrosion and wear protection. Manufacturing was performed with traditional methods, such as flame and plasma spraying. Later, thermal spray technologies were developed, and interest increased in producing polymer or polymer-composite coatings from different polymer materials with advanced spray processes. Additionally, novel application fields were studied, such as the use of thermally sprayed polymer coatings for anti-icing and anti-fouling purposes. This review summarizes thermally sprayed polymer coatings from the standpoints of materials, processes used and selected latest application fields.

**Keywords** anti-fouling · anti-icing · cold spraying · corrosion protection · flame spraying · polymer coating · thermal spraying

## Introduction

Polymer coatings have been manufactured by thermal spraying for decades, and development has continued to date. Thermal spray processes have been modified to

improve coating processability, and feedstock materials have been developed and tailored to achieve better performance. An important application field for thermally sprayed polymer coatings is used as protective layers to address several conditions. Petrovicova and Schadler (Ref 1) summarized the most important advantages of thermally sprayed polymer coatings over other polymer coatings; this included environmental aspects, such as obviating the need for solvent systems containing volatile organic compounds. Other advantages were related to ease of manufacturing as well as suitability for coating onto large surfaces, the use of different processing conditions and development of materials exhibiting high viscosities. Petrovicova and Schadler (Ref 1) published their review on thermal spraying of polymers almost twenty years ago, so it is now appropriate to review the state-of-the-art for thermally sprayed polymers and polymer-based coatings again.

Thermal spray processes for polymer coating production include flame spraying, high-velocity oxygen fuel (HVOF)/high-velocity air fuel (HVOF), plasma spraying (Ref 1) and cold spraying. Figure 1 summarizes the main factors affecting thermal spray processes, which depend on and vary with the process, the polymer material and the substrate conditions. Many factors must be taken into account when optimizing thermal spray processing with polymer and polymer-based coatings. Flame spraying is a thermal spray technology used for production of polymer coatings. Polymeric feedstock material is fed to the gun, melted, and accelerated toward the substrate surface, and the particle velocity can reach approximately 50–100 m/s (Ref 2). One advantage of flame spraying is that it can be used on site, so it is a very flexible processing method. Earlier flame spraying was done manually, whereas current processes are more automated due the use of robotics. Flame-sprayed polymer coatings used to protect pipelines from corrosion

---

This invited article is part of a special issue focus in the Journal of Thermal Spray Technology celebrating the 30th anniversary of the journal. The papers and topics were curated by the Editor-in-Chief Armelle Vardelle, University of Limoges/ENSIL.

---

✉ Heli Koivuluoto  
heli.koivuluoto@tuni.fi

<sup>1</sup> Faculty of Engineering and Natural Sciences, Materials Science and Environmental Engineering, Tampere University, Tampere, Finland

have included polyethylene (PE) coatings with thicknesses of 1-3 mm (Ref 3, 4). Additionally, HVOF, plasma spraying, and cold spraying have been used to produce polymers or polymer-based coatings.

In addition to PE, thermal spraying has been used to produce coatings comprising polypropylene (PP) (Ref 5), polyethylene terephthalate (PET) (Ref 6), polyamide (PA) (Ref 7), polyether sulfone (PES) (Ref 8), polycarbonate (PC) (Ref 1), polyphenylene sulfide (PPS) (Ref 1), polytetrafluoroethylene (PTFE) [9], polyether ether ketone (PEEK) (Ref 7, 10), polyimide (PI) (Ref 7), polyvinyl chloride (PVC) (Ref 5–11), polyvinylidene fluoride (PVDF) (Ref 12), ethylene chlorotrifluoroethylene (ECTFE) (Ref 12), perfluoroalkoxy alkane (PFA) (Ref 12), fluorinated perfluoroethylenepropylene (FEP) [Ref 13], ethylene methacrylic acid (EMAA) (Ref 14), polystyrene (PS) (Ref 15) and the copolymers ethylene vinyl acetate (EVA) and ethylene vinyl alcohol (EVAL) with PE (Ref 16). Polyethylene is one of the most common polymers used in thermal spraying. It has been used in powdered forms with different densities, such as low-density polyethylene (LDPE) (Ref 17), high-density polyethylene (HDPE) (Ref 15), and ultrahigh molecular weight polyethylene (UHMWPE) (Ref 18). Polymers are materials that consist of organic compounds, and they can be produced synthetically or transformed from natural products. Thermoplastics, in turn, are physically linked macromolecules with linear or branched bonds, whereas elastomers and thermosets are cross-linked. Thermoplastics can be crystalline, semicrystalline or amorphous (Ref 11). When thermoplastics are heated, they can soften and flow. For

example, PE and PS are thermoplastics (Ref 11, 19). When they are cooled, they harden. In addition, this processing can be repeated (Ref 9), and these materials are therefore suitable for thermal spraying.

Table 1 shows some examples of materials, and the melting points are relatively low compared to those of other thermally sprayable materials, such as metals, hard-metals and ceramics. Thermal spraying of polymers can be performed, but it requires process optimization, modification and more temperature control than processes for other materials. By using optimized process parameters, degradation can be avoided. Several studies have reported no detectable deterioration (Ref 14, 20) or minimal degradation by using Fourier transform infrared spectroscopy (FTIR) (Ref 21).

Thermally sprayed polymer coatings are protective, but they are inexpensive and easy to manufacture (Ref 1, 24). For example, thermally sprayed polymer coatings have been considered for corrosion protection, and biocompatible polymer coatings have been studied as potential solutions for problems in the medical sector. Additionally, thermally sprayed polymer coatings have been investigated for low-friction applications and wear protection. In this case, high-performance polymers were used, e.g., PEEK (Ref 25). One way to enhance the mechanical properties of thermally sprayed polymer coatings is by adding reinforcement agents that act as polymer nanocomposite coatings (Ref 26). The latest application fields under study are focused on protecting against environmental stresses such as icing (Ref 5) and fouling (Ref 2).

**Fig. 1** Summary of factors influencing thermal spray processing of polymer powders. Modified from (Ref 1), reprinted by permission of Taylor & Francis Ltd.

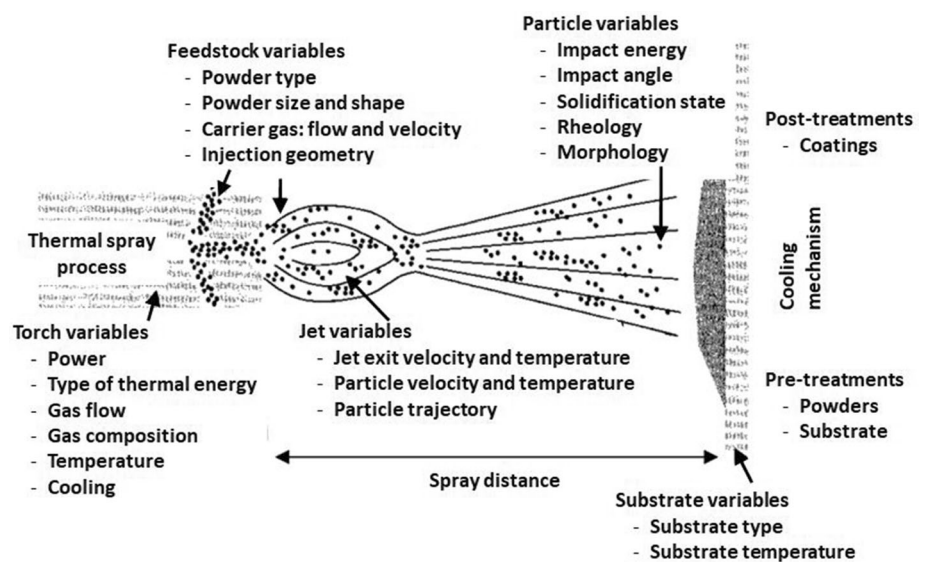


**Table 1** Melting points of polymer materials used in thermal spraying

Polymer	Melting point, °C	References
Polyethylene, PE	140	19
Polypropylene, PP	176	19
Polyvinyl fluoride, PVF	200	19
High-density polyethylene, HDPE	128	22
Polyurethane, PU	92	22
Polyamide, PA	180	22
Polystyrene, PS	175	22
Ultrahigh molecular weight polyethylene, UHMWPE	130	22
Polyethylene terephthalate, PET	243	23
Polyvinylidene fluoride, PVDF	155-170	12
Ethylene chlorotrifluoroethylene, ECTFE	240	12
Perfluoroalkoxy alkane, PFA	300-310	12
Fluorinated perfluoroethylenepropylene, FEP	250-280	12
Ethylene methacrylic acid, EMAA	80-105	20

## Flame Spraying of Polymer Coatings

Flame spraying is the most common thermal spray process used for production of polymer coatings. More information on flame spraying and other thermal and cold spray processes used in coating production can be found (Ref 1, 4). There are special flame spray guns available for polymer spraying, as well as tailored systems, to manufacture coatings from hybrid feedstock materials. Flame-sprayed methacrylic acid (MAA) PE coatings have been studied for protection of steel substrates from corrosion. The typical particle size of the PE powder was 149  $\mu\text{m}$ , and propane was used as a fuel gas. Adhesion between the coating and substrate was influenced by processing parameters such as gas and air pressures, as well as the traverse speed of the gun. Additionally, it has been reported that cathodic delamination (corrosion resistance) is correlated with adhesion; i.e., higher adhesion leads to better corrosion resistance (Ref 2). Flame-sprayed PE (FS PE) coatings have shown potential for use in anti-icing applications. Hydrophobic and icephobic FS PE coatings have been produced by using flame spraying with an acetylene-oxygen flame (Ref 5, 21, 28). Processing parameters influenced the properties of flame-sprayed polymer coatings. For example, the coating thickness increased with increasing spraying distance when slow a traverse speed was used (Ref 21). Another approach for thermally sprayed PE coatings was the production of porous PE structures by using flame spraying with an acetylene-oxygen flame. These porous structures have been impregnated with a lubricant to act as slippery liquid infused porous surfaces (SLIPS). In this way, slippery surfaces can be produced, and high icephobicity can be achieved due to the slipperiness of the surface (Ref 29).

Flame spraying of amorphous PEEK for wear protection and friction reduction has been studied. In this case, the particle sizes were much lower than 25  $\mu\text{m}$ . The metal substrate was preheated prior to coating production, and the sample was quenched after spraying. As a result, the semicrystalline coating had higher hardness and expected improved wear and friction properties (Ref 25). Furthermore, Soveja et al. (Ref 30) observed that an FS PEEK coating could be densified by using laser treatment as a remelting process. In addition to providing the denser coating structure, laser treatments improved the adhesion between FS PEEK and the steel substrate due to fusion of the polymer. As noted, flame spraying of PEEK requires specific preheating or posttreatment to ensure successful production of the coating. A key factor was a low processing temperature, which was enabled by process and nozzle development. In this way, a dense PEEK coating (Fig. 2) was produced for corrosion protection (Ref 10). Dense FS PEEK and PEI and PA coatings have been produced by Lima et al. (Ref 7). The surface and structure of flame-sprayed PE and PE composite coating containing natural components from capsaicin are presented in Fig. 3. Additionally, dense PE-based coatings have been produced, showing successful tailoring of coating structures by modifying the feedstock material (Ref 27).

In addition to those on PE and PEEK, investigation of the flame-sprayed fluoropolymer PVDF, ECTFE, PFA and FEP coatings showed their dense and smooth coatings, which were beneficial for corrosion protection (Ref 12). Flame-sprayed EMAA splats (Ref 14) and PP splats (Ref 31) were studied to evaluate the influence of process parameters on splat formation. For example, spray distance influenced the flattening of EMAA particles, and the useable distance range depended on the substrate material. A higher spray distance can be used for glass substrates than

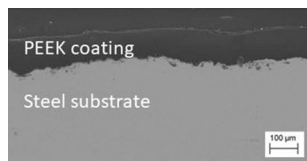


**Fig. 2** Flame-sprayed PEEK coating on steel substrate. Modified from (Ref 10)

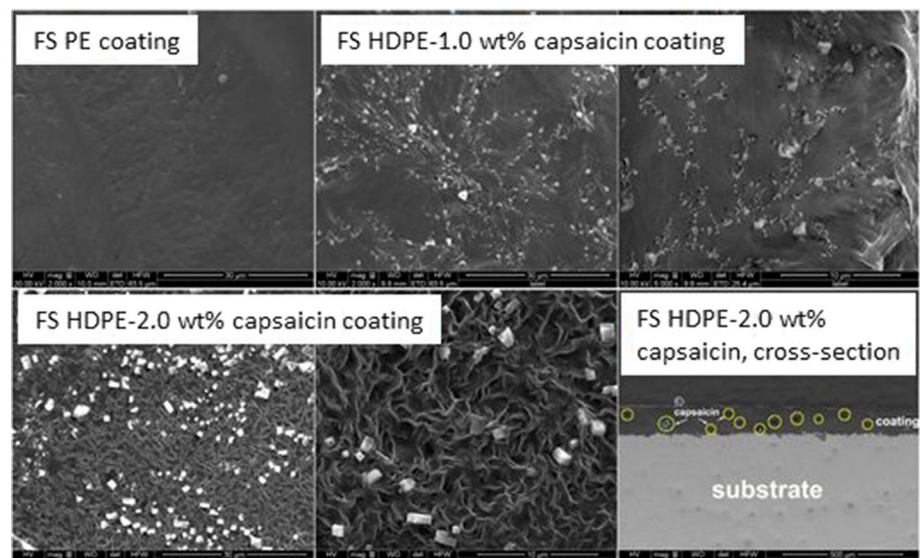
for steel substrates (Ref 14). Flattening of FS EMAA splats on glass substrate increased up to a distance of 30 cm, whereas the distance limit for steel substrates was 25 cm, as reported by Xie et al. (Ref 14). This has been explained by a higher splat temperature on the steel substrate, which in turn was due to the higher thermal conductivity of steel compared with glass (Ref 14). Recently, liquid flame spraying (Ref LFS) of polymers has been introduced by using precursors (Ref 32) or suspensions (Ref 3) as feedstock materials. When a feedstock in liquid form is fed to the flame spray gun, it must be synthesized by the flame and then sprayed on the substrate surface (Ref 3). Wang et al. (Ref 32) used an oxygen-acetylene flame with LFS of PI and PI with Cu coatings. Liu et al. (Ref 33) studied suspension flame spraying to produce PI-Cu coatings for anti-fouling and anti-corrosion purposes by combining the functional effects of both organic and inorganic materials in the composite structure.

Flame spraying of HDPE and HDPE with Cu has also been studied for anti-fouling and anti-corrosion purposes. This approach was used for the manufacturing homogenous and dense HDPE + Cu coatings from Cu-coated HDPE particles (Ref 34). In addition, FS HDPE and HDPE + Cu coatings have been studied for anti-aging protection (Ref 35). Aging was performed with a xenon lamp, and the HDPE + Cu coatings showed better aging resistance than

the HDPE coating due to the inclusion of Cu. Additionally, Liu et al. (Ref 27) used flame spraying to produce composite coatings with HDPE and capsaicin for anti-fouling purposes. Furthermore, PHBV/50PMMA coatings for biomedical purposes have been produced with oxygen-acetylene flame spraying. Flame spraying has enabled the production of hydrophilic and biocompatible polymer coatings for drug delivery systems after implant surgery (Ref 36). Flame-sprayed maleic anhydride (MAH)-grafted (g)-LDPE and MAH-g-LDPE/UHMWPE composite coatings have been produced for corrosion protection and further blended with nanocomposite coatings (MAH-g-LDPE/UHMWPE); they showed better corrosion resistance, whereas abrasion resistance was higher with MAH-g-LDPE (Ref 37). Additionally, a flame-sprayed grafted maleic acid (MAc) LDPE coating showed higher adhesion than a flame-sprayed LDPE coating (Ref 17). Li et al. (Ref 3) studied flame-sprayed PEEK with CNTs, which exhibited high coating quality and high tribological performance due to improved lubrication provided by the CNTs and therefore better results in wear tests. Application of PEEK/CNT powder with an ultrasound dispersion method provided denser coatings than mechanically blended powders. Higher splatting of PEEK was thought to be the reason for enhanced performance of the powder applied with ultrasound dispersion (Ref 38).

Flame spraying of PA, HDPE and PET was performed with an air-propane flame spray gun (Ref 24). Here, heat generation can be varied with the nozzle design, as shown in Fig. 4. By changing the combustible mixture exiting from the central part (V) and using additional air flow ( $V_g$ ), the flame shape can be changed, which, in turn, influences the formation of the coating and the resulting properties (Ref 24). The flame can generate oxidizing, stable or reducing

**Fig. 3** Surfaces and structures of flame-sprayed PE and PE + capsaicin coatings. Modified from (Ref 27), reprinted with permission from Elsevier



conditions depending on the gas-air mixture ratio (Ref 39). For example, FS PA coatings show higher adhesion when sprayed with an oxidizing flame. Improved coating-substrate adhesion was explained by the high number of oxygen-containing groups formed on the polymers due to oxidizing flame conditions (Ref 24)

Table 2 provides an overview of polymer coatings produced with flame spraying. Work on the development of thermally sprayed polymer coatings and polymer-composite coatings mainly occurred in the 2000 century. Several different polymer materials and protective purposes have emerged as features of flame-sprayed polymer coatings. Additionally, tailoring of feedstock materials has enabled the production of polymer-based composite coatings with important properties.

### High-Velocity Flame Spraying of Polymer Coatings

This section is focused on polymer coatings made with high-velocity flame spraying, and more information on the process itself is presented in (Ref 1, 4). PET coatings have been produced via high-velocity oxygen fuel (HVOF) spraying (Ref 6). This indicated crystallization of the amorphous feedstock during thermal spraying. However, later melting and quenching decreased the extent of crystallization. Heat-treated thermally sprayed PET coatings exhibited better tribological properties than PET because they showed lower friction and wear rates (Ref 6). In another study, a PET coating was successfully deposited by using a low-velocity oxygen fuel (LVOF) process; this prevented corrosion by gasoline, diesel oil and alcohol and confirmed the potential for use these coatings as corrosion barriers in fuel tanks (Ref 3). Figure 5 shows the structures of LVOF PET coatings on a steel substrate. When the substrate was not preheated, a layered structure resulted, and adhesion was poor. Preheating of the substrate improved adhesion between the coating and the substrate,

but more bubbles were formed inside the coating structure at higher temperatures. This was attributed to greater degradation of PET caused by higher temperatures (Ref 23). The coefficient of friction for a HVOF PA coating with silica was lower than that for a HVOF PA coating, which was possibly due to crystallinity (Ref 47). The mechanism for wear of the polymer coating in sliding wear was identified as smearing, whereas other wear mechanisms also include abrasive and fatigue wearing of polymer-composite coatings (Ref 47).

Single splat tests for PEEK particles were performed with HVOF and assisted combustion high-velocity air fuel (AC-HVAF) by evaluating the effects of surface roughness and chemistry on particle bonding (Ref 4). The skewness of a substrate surface has a significant effect on splat formation, although the surface roughness values were at the same level. This skewness indicated the shapes of peaks and valleys and, whether the shapes were blunt or sharp, which cannot be seen from the roughness itself. Positive skewness, where roughness peaks were sharp, increased the contact areas for the splats and improved mechanical interlocking (Ref 8). Additionally, HVAF-sprayed PEEK splats were studied by Withy et al. (Ref 49) who showed that the surface chemistry and roughness of the substrate strongly affected splat formation, whereas Patel et al. (Ref 48) noticed that the amount of PEEK particles was higher on grit-blasted steel than on etched steel and lowest on degreased steel. In addition to roughness, skewness was also found to affect adhesion of PEEK particles on steel substrates at room temperature. The positive skewness of the substrate surface increased adhesion because the areas available for mechanical interlocking were increased (Ref 48). More HVAF PEEK splats were bonded to the polished substrate and the polished and thermally treated aluminum substrate than to etched and boiled substrates with and without thermal treatment (Ref 49).

HVOF ceramic/polymer (silica/nylon) coatings have been studied to determine wear resistance. The powders used had a nylon core and shells with embedded silica

**Fig. 4** Flame shapes with different nozzle designs. Modified from (Ref 24), reprinted with permission from AIP Publishing

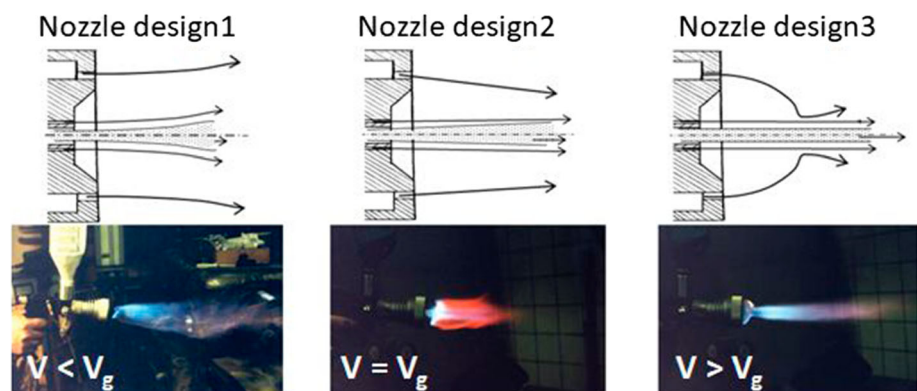


**Table 2** Summary of flame-sprayed (FS) polymer coatings and their purposes and performances

Coating material	TS-process	Purpose/properties	Findings/performance	Reference (Publication year)
MA-modified PE	FS (propane/air)	Deposition on steel substrate, effect of process parameters	Higher bond strength led to a lower delamination rate in corrosion studies.	Ref 2 (1995)
PVDF, ECTFE	FS (oxygen/acetylene, air/propane)	Dense and smooth coatings	Corrosion protection	Ref 12 (2004)
LDPE LDPE-g-MAc	FS (acetylene/air)	Improved adhesion with maleic acid crafting	Corrosion protection	Ref 17 (2007) Ref 40 (2011)
EVA, EVA1 + PE	FS	EVA/PE coatings high corrosion resistance in sea water conditions	Anti-corrosive coatings	Ref 16 (2010)
PP	FS (acetylene/oxygen)	Splats on glass	Understanding of splat formation and flattening	Ref 31 (2010) Ref 41 (2011)
Epoxy	FS (acetylene/air)	Flame spraying of thermoset powders. Modeling of cure kinetics.	Additional heating to cure the epoxy. Curing rate models as process control	Ref 42 (2012)
PHVB/PMMA	FS (oxygen/acetylene)	Adhesion depends on spray parameters, hydrophilic coatings	Biocompatible polymer coatings for drug delivery systems	Ref 36 (2012)
EMAA, EMAA/ZrO <sub>2</sub> , EMAA/Al <sub>2</sub> O <sub>3</sub>	FS (propane/air, acetylene/oxygen)	Splats on heated and unheated mild steel and glass	Substrate chemistry affected splat morphology, more amorphous when sprayed with acetylene rather than propane	Ref 20 (2013)
EMAA	FS (propane/air)	Splats on mild steel	Effect of spray distance on splat flattening, no degradation	Ref 20 (2013) Ref 14 (2014)
PA + PU microcapsules	FS with additional feeding for capsules	Liquid–solid lubrication with flame spraying	Low-friction coatings with self-lubricating and self-healing properties	Ref 43 (2013)
PEI, PEEK, PA	FS (acetylene/Oxygen)	Dense and smooth coatings, good adhesion	Better wear and corrosion performance for PA than PEEK, and weakest for PEI	Ref 7 (2013) Ref 44 (2016)
LDPE	FS (acetylene/oxygen)	Low or medium-low ice adhesion	Anti-icing coatings	Ref 28 (2017) Ref 29 (2018) Ref 21 (2020) Ref 5 (2020)
PP, PE + FEB, PEEK, UHMWPE	FS (acetylene/oxygen)	Low, medium-low or medium ice adhesion	Anti-icing coatings	Ref 5 (2020)
PEEK	FS	Coatings' crystallinity and hardness increased with heat treatment	Mechanical and tribological performance, heat treatment lowered friction and wear rate	Ref 10 (2020)
LDPE + solid lubricants	FS (acetylene/oxygen)	Low ice adhesion, resistant to corrosive medias	Anti-icing coatings	Ref 45 (2020) Ref 46 (2021)
PEEK + CNTs (carbon nanotubes)	FS (acetylene/oxygen)	Powder blending using mechanical blending and ultrasound dispersion	Ultrasound dispersion resulted in denser coatings and better tribological performance	Ref 38 (2022)

**Fig. 5** Structures of LVOF-sprayed PET coatings produced on steel substrates with different preheating temperatures, including no preheating and preheating at 170, 200 and 215 °C. Modified from (Ref 23), reprinted with permission from Elsevier

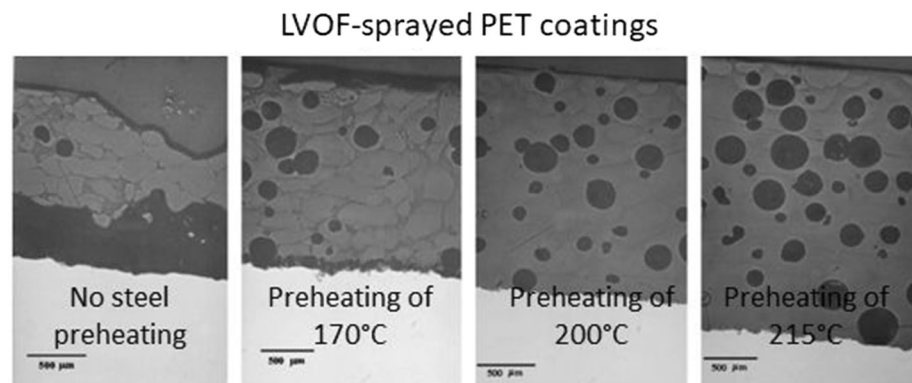


**Table 3** Summary of high-velocity oxygen fuel (HVOF) and plasma-sprayed polymer coatings and their purposes and performance

Coating material	TS-process	Purpose/properties	Findings/Performance	Reference (Publication year)
PA, PA + fumed SiO <sub>2</sub>	HVOF (hydrogen/oxygen)	Sliding wear properties, substrate steel	Improved wear resistance with nanoceramic particles	Ref 50 (1997) Ref 47 (2007)
PMMA	Plasma spray (argon/hydrogen, nitrogen-hydrogen)	Effect of gun speed and gas composition	Decomposition increased with large temperature gradients; wear resistance improved with high torch speed	Ref 52 (1997)
PET	HVOF (Kerosene)	Thickness ~ 350 µm, low friction of coefficient	Heat-treated coatings had better wear resistance compared to PET bulk material	Ref 6(1999)
PET	Low-velocity oxygen fuel (LVOF) spray (propane, oxygen, air)	Role of substrate preheating to characteristics of the coatings	Higher preheating temperature, higher degradation but also higher adhesion	Ref 23 (2004)
PVDF, ECTFE, PFA, FEP PFA + ceramics PTFE + ceramics	Plasma spray (argon/hydrogen) Plasma spray (argon/hydrogen)	Dense and smooth coatings Homogenous composite coating with modified powder feeding	Corrosion protection Improved wetting behavior and lower friction coefficient	Ref 12 (2004) Ref 53 (2005) Ref 54 (2006)

particles, as well as pure nylon particles alone. Wear resistance was greater for the silica/polymer coating compared with the pure polymer coating due to the chemical changes caused by adding nanosized ceramic fillers (Ref 50). Additionally, HVOF spraying was used to produce polymer (nylon 11) nanodiamond composite coatings. Nanodiamond addition improved adhesion of the coating by densifying the structure. Hard nanodiamonds reinforced the composite coating structure and coating–substrate interface (Ref 51). Table 3 presents a summary of HVOF and plasma-sprayed polymer coatings. The latest developments have been focused more on flame spraying (Table 2) and cold spraying (Table 4) than on high-velocity processes or plasma spraying. However, HVOF and plasma-sprayed polymer coatings have primarily been studied for wear resistance.

### Plasma Spraying of Polymer Coatings

Plasma spraying of fluoropolymers, PVDF, ECTFE, PFA and FEP powders (Ref 12) and ceramic/fluoropolymers (Ref 54) has been studied. More details on the process of plasma spraying can be found in (Ref 1, 4). Plasma spraying has been used to produce polymer-steel coatings for low-friction applications. In this case, plasma spraying was used to apply a thin polymer coating on a plasma-sprayed steel coating to improve lubrication. Thin plasma-sprayed coatings were made from PA, PA with solid lubricant, UHMWPE, UHMWPE with solid lubricant, PTFE and PTFE with PA. Both MoS<sub>2</sub> and graphite additives were tested. The best wear performance was achieved with pure PA (nylon 11) as the top coating, whereas a continuous coating of plasma-sprayed PTFE could not be produced. All plasma spray process parameters used degraded PTFE particles, which resulted in poor adhesion

**Table 4.** Summary of cold-sprayed polymer coatings and their purposes and performance

Coating material	TS-process	Purpose/properties	Findings/performance	Reference (Publication year)
HA-Ag/PEEK	Cold spray (air)	Successful deposition of composite coatings	Antibacterial coatings	Ref 56 (2009)
Chitosan-Cu/Al	Cold spray (He)	Successful deposition of composite coatings	Antibacterial coatings, deposition of biopolymer with metallic powders	Ref 57 (2009)
PE	Cold spray (air)	Numerical and experimental studies (CFD models, Schlieren photos)	Nozzle development for polymer coating production. No melting of polymer particles.	Ref 58 (2012)
UHMWPE, UHMWPE + nano-Al <sub>2</sub> O <sub>3</sub> /fumed nano-Al <sub>2</sub> O <sub>3</sub> -SiO <sub>2</sub>	Low-Pressure Cold spray (air)	Effect of addition of ceramic particles on polymer coatings. Nozzle optimization.	Thick UHMWPE+nano-Al <sub>2</sub> O <sub>3</sub> coatings on Al and PP substrates	Ref 59 (2015)
PE-CNT	Low-pressure cold spray (air)	Spraying on PP and porous structured aluminum	Successful deposition, PE melted in CS process and CNTs adhered on those. Electrical conductivity.	Ref 60 (2017)
HDPE	Custom-made cold spray (air)	HDPE coatings on polymer substrates and on Al and quartz glass.	Effect of process parameters. DE increased with increased particle temperature, impact velocity and substrate temperature.	Ref 61 (2017)
UHMWPE-FNA (fumed nano- Al <sub>2</sub> O <sub>3</sub> )	Low-pressure cold spray (air)	Production of polymer-ceramic composite coatings	DE increased with increasing amount of FNA	Ref 18 (2018)
HDPE, PU, PA, PS, UHMWPE	Laboratory-scale cold spray (nitrogen, air)	Particle impact velocities of polymers, decreased critical velocities with increasing temperatures	Low porosity coatings with optimized spray parameters. Possibilities for 3D additive manufacturing of polymer parts	Ref 22 (2020)
UHMWPE	Cold spray, modeling	Particle inflight properties such as temperature and velocity	Simulation of impacts during cold spraying	Ref 62 (2020)
FEP, FEP + nanoceramic	Low-pressure cold spray (air)	Wetting performance of coatings	Superhydrophobic cold spray coatings, low roll-off contact angles	Ref 13 (2020)
HDPE, PU, PA, PS, UHMWPE	Laboratory-scale cold spray (air)	Effect of glass peening particles on polymer coatings	Increased DE by using glass beads mixed with polymer powders	Ref 15 (2020)
PEEK	Cold spray	Modeling of PEEK particles in cold spraying	Numerical investigations of CS PEEK on PEEK. Narrow particle velocity range for successful deposition	Ref 63 (2021)

(Ref 9). Wu et al. (Ref 55) evaluated plasma-sprayed PEEK splats and concluded that the surface chemistry of the aluminum substrate was more important in determining particle bonding than the roughness of the surface. Plasma spraying has been used to manufacture electromagnetically absorbing coatings from hexaferrite and polyester (Ref 8). Good electromagnetic properties of the composite coatings

were achieved by coupling the magnetic and dielectric losses of hexaferrite with the dielectric losses of polyester (Ref 8). Examples of plasma-sprayed composite coatings are presented in Fig. 6. Plasma-sprayed PMMA coatings showed increased decomposition with increasing process temperatures. Additionally, other process parameters affected the plasma-sprayed PMMA coatings. For example,



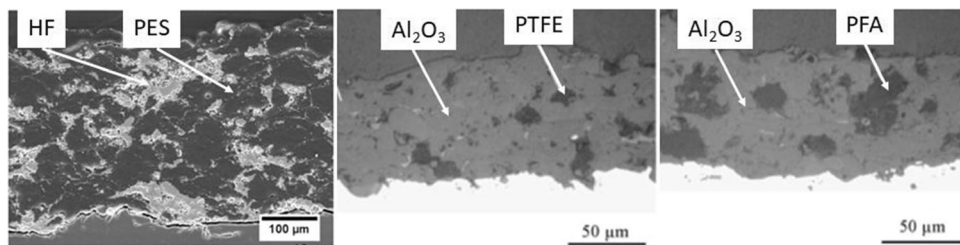


**Fig. 6** Structures of plasma-sprayed hexaferrite/polyester (HF/PES) (Ref 8), alumina/polytetrafluoroethylene ( $\text{Al}_2\text{O}_3\text{-TiO}_2\text{/PTFE}$ ) (Ref 53) and alumina/tetrafluoroethylene-co-perfluoropropylvinylether

( $\text{Al}_2\text{O}_3\text{-TiO}_2\text{/PFA}$ ) (Ref 53) coatings. Modified from (Ref 8), reprinted by permission from Springer Nature. Modified from (Ref 53), reprinted with permission from Elsevier

a coating sprayed with a faster gun speed resulted in a lower wear rate compared to a coating produced with a slower gun speed. Degradation was lower with faster application speeds, which, in turn, led to better wear resistance (Ref 52).

### Cold Spraying of Polymer Coatings

Research on cold spraying of polymers has been active, and several polymeric materials have been successfully produced by using the cold spraying process. Table 4 summarizes cold-sprayed polymer and polymer-based composite coatings and their purposes. Figure 7 shows some of the powders used, and the powder morphologies varied from spherical to very irregular. One challenge for polymer application by cold spraying, as well as for other thermal spray processes, is the availability of suitable powders. Therefore, processing must be done with the powders available, but these are not optimized for the thermal and cold spray processes. Successful coatings have been produced, but even more improved coating properties could be achieved with optimized powders and optimized processes.

Some studies have been focused on spraying single particles and analyses of single particle interactions with the substrate. Additionally, the thermal history of the powder and its influence on cold-sprayed polymer coatings

have been modeled, and these showed that the thermal gradient for the powder depended on the particle size (Ref 62). For example, single PS and PA particles were successfully sprayed on LDPE substrates (Fig. 8) by using single particle microballistic experiments as models for cold spraying (Ref 64). Another study was focused on cold spraying of PEEK onto a PEEK substrate. It was observed that small particles had higher critical velocities (360 m/s for 10  $\mu\text{m}$ ), whereas medium-sized particles had critical velocities 257 m/s (40  $\mu\text{m}$ ) and large particles again had higher critical velocities (277 m/s) (Ref 63). The velocities of polymer particles used for successful coating were much lower than those of metal particles (Ref 6).

Chitosan polymer has been studied with cold spraying, and it was blended with Cu/Al. Chitosan is a natural polymer that is both biocompatible and nontoxic. Interest in this material has increased due to its biodegradability (Ref 57). There are also other studies on cold-sprayed composite coatings in which polymers were one of the composite contents. For example, HA-Ag/PEEK coatings have been applied with cold spraying, and antibacterial properties have been the driving force for use of these coatings. The process gas was air, and it was preheated to 150–160  $^\circ\text{C}$ . Coatings were produced successfully and showed high biofunctionality similar to that of the starting material (Ref 56).

Ravi et al. (Ref 18, 59) studied cold spraying of UHMWPE and UHMWPE with alumina nanoparticle powders. A low-pressure cold spray (LPCS) system was used with a pressure of 2–8 bar and temperatures of RT–500  $^\circ\text{C}$  (air). In this study, it was determined that the polymer needed thermal softening to enable successful bonding, and therefore, the process was optimized by using a longer nozzle to achieve sufficient thermal softening. Figure 9 shows SEM cross sections of LPCS UHMWPE coatings on Al and PP substrates. Even behavior-level thick UHMWPE + alumina nanoparticle coatings were produced with LPCS methodology (Ref 59). Additionally, UHMWPE mixed with nanoalumina, fumed nanoalumina and fumed nanosilica has been applied with cold spraying (Ref 65). The coating thicknesses varied for the different

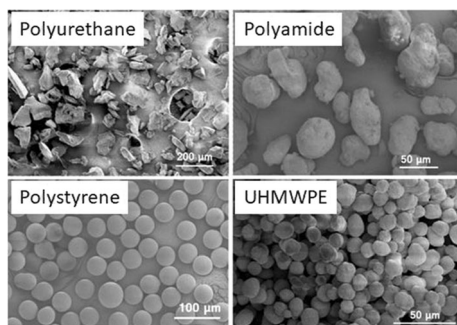


**Fig. 7** Polymer powder morphologies used in cold spraying. Modified from (Ref 22), reprinted with permission from Elsevier

**Fig. 8** SEM images of single PS and PA particles deposited on a LDPE substrate. The impact velocity for PS was 290 m/s, and that for PA was 355 m/s. Modified from (Ref 64), reprinted with permission from Elsevier

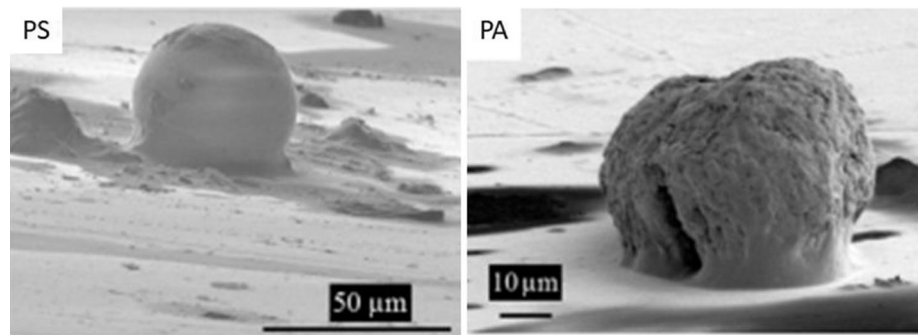
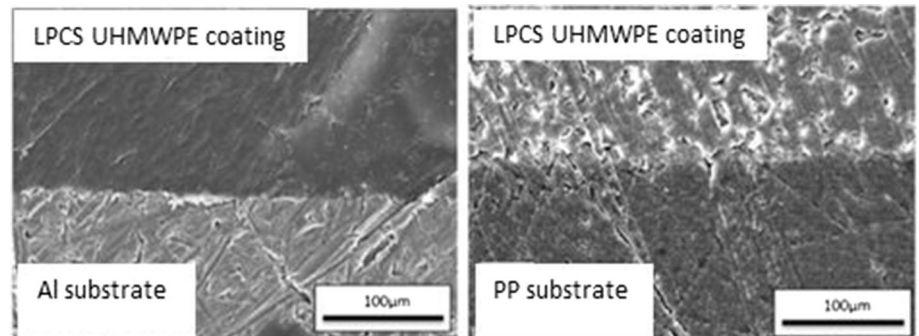


**Fig. 9** LPCS UHMWPE coatings on Al and PP substrates. Modified from (Ref 59), reprinted by permission from Springer Nature



powders. The thicknesses of the coatings were 1–4 mm for UHMWPE, 70–100  $\mu\text{m}$  for HMWPE-nanoalumina and 70–150  $\mu\text{m}$  for UHMWPE-nanosilica. Nanoceramic particles strengthened the structures of the composite coatings by reinforcing bonding between polymer particles. This has been explained by noting that nanoparticles were located near the polymer particles and activated bonding during impact because of their surface chemistry (hydroxyl groups) (Ref 65).

LPCS PFA and PFA with fumed nanoalumina (FNA) as a core-shell coating are hydrophobic, and furthermore, LPCS PFA-FNA coatings on laser-textured steel substrates have shown superhydrophobic wetting behavior (Ref 26). These findings showed that cold spraying is a fast and one-step coating process for producing superhydrophobic polymer-based composites (Ref 26). The hydrophobicities of cold-sprayed coatings have been of interest, and for that purpose, cold spraying of fluoroethylene propylene (FEP) powders and those with added fumed nanoceramic (FNC) hydrophobized silica and alumina have been studied by Lock Sulen et al. (Ref 13). They used LPCS equipment to fabricate hydrophobic CS FEP coatings on an aluminum substrate. Hydrophobicity was further improved with the addition of hydrophobized FNC to the FEP powder.

The use of optimized nozzles for successful deposition of cold-sprayed PE on an Al-alloy substrate is confirmed by modeling and experimental work (Ref 58). In addition, the cold spray process was used to successfully produce PE-carbon nanotube (CNT) coatings on PP and nanoporous

structured aluminum substrates. In this study, PE particles were melted during the CS process and CNTs were bonded to the melted PE. These CS PE-CNT coatings were shown to be electrically conductive (Ref 60).

Bush et al. (Ref 61) studied the effects of several process parameters on the cold spraying of HDPE powder. The parameters considered were particle temperature, size and impact velocity, as well as nozzle design, spray distance and substrate composition and temperature. The deposition efficiencies of polymer powders can be improved by selecting optimal spray parameters. The critical velocities for polymers have been reported to be lower than those for metals because of the lower particle temperatures and different thermal diffusivities of polymer particles

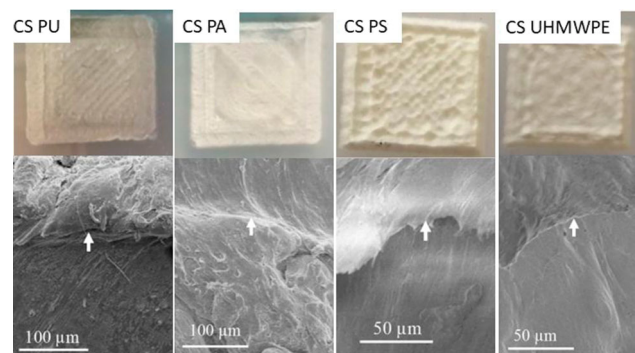


**Fig. 10** Cold-sprayed PU, PA, PS, and UHMWPE coatings. The arrows show the interfaces. Modified from (Ref 22), reprinted with permission from Elsevier

compared to metal particles. Furthermore, the efficiencies for deposition of CS HDPE powders were much lower than those for metal powders (Ref 61). Cold-sprayed HDPE, PU, PS, PA, and UHMWPE coatings were produced successfully, and the structures are shown in Fig. 10 (Ref 22). Furthermore, polymeric materials have been sprayed together with glass beads to improve the properties of cold-sprayed polymer coatings. The deposition efficiency increased with the use of peening particles, which also made the coating smoother and the structures more uniform (Ref 15).

## Selected Application Fields for Thermally Sprayed Polymer Coatings

### Anti-icing

FS PE (Ref 21, 28) and PE+FEB coatings have shown low or medium-low ice adhesion with high durability. Furthermore, the ice adhesion of FS PE and PE+FEB can be decreased by polishing the surfaces. Figure 11 shows the low ice adhesion seen for a FS PE coating compared to stainless steel, aluminum and polyurethane paint, indicating that ice removal from the surface was improved. In addition, these coatings exhibited hydrophobic wetting performance, which was beneficial for icephobicity. Low ice adhesion is needed for anti-icing purposes (Ref 28). Thermally sprayed slippery liquid infused porous surfaces

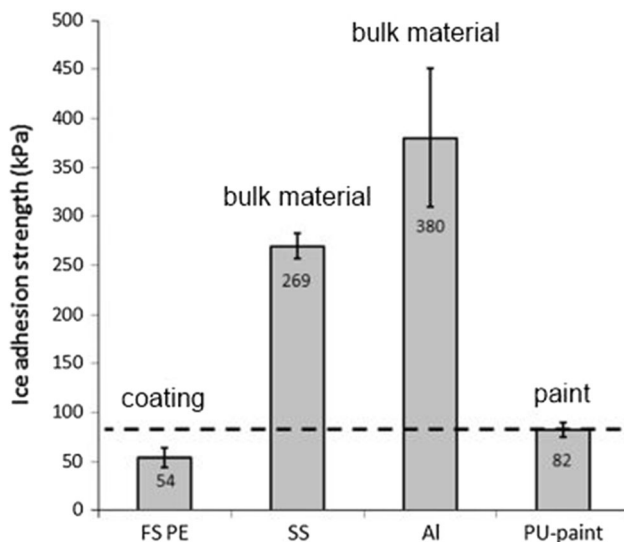


**Fig. 11** Ice adhesion values (a) for flame-sprayed PE coating (FS PE), stainless steel (SS) and aluminum (Al) bulk materials and polyurethane paint (PU paint), modified from (Ref 28), reprinted by permission from Springer Nature and (b) for stainless steel, PU paint, SLIPS and thermally sprayed dense coating (TS dense), and rough and smooth TS-SLIPS, modified from (Ref 29). All results were measured with the same centrifugal ice adhesion testing device

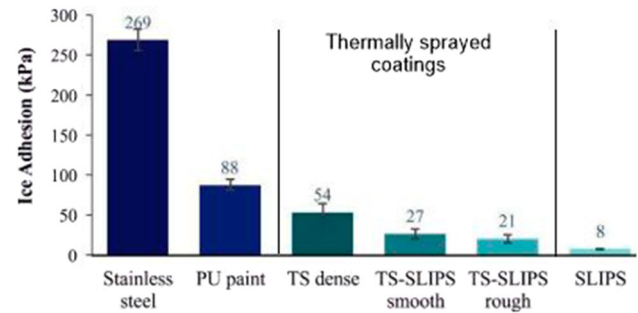


**Fig. 11** continued

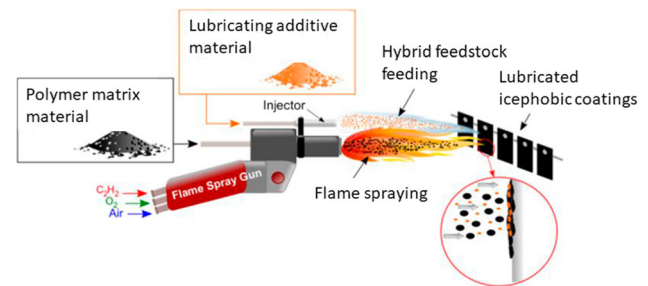


**Fig. 12** Advanced flame spraying with injection of a hybrid feedstock to produce a lubricated icephobic coating (LIC). Modified from (Ref 45)

(TS-SLIPS) have shown very low ice adhesion and can be called novel icephobic solutions (Ref 29). Donadei et al. (Ref 21) showed that process parameters influenced thermal degradation, which in turn, affected ice adhesion. Lower thermal degradation led to lower ice adhesion. This was achieved by increasing the traverse speed of the spray gun (Ref 21).

In another study, Donadei et al. (Ref 45) modified flame spraying by adding hybrid feedstock injection to produce lubricated icephobic coatings (LICs). A heat-sensitive additive material was fed with an additional feeder outside the flame, while PE powder was fed traditionally through the spray gun Fig. 12. Lubricating additives were distributed in the PE matrix coating and increased the slipperiness of the coating. LICs were hydrophobic and icephobic and provided high water repellence and anti-icing performance, respectively Ref 45.

### Anti-fouling

Liquid flame spraying (LFS) has been used to produce PI-Cu coatings exhibiting anti-fouling behavior. Interestingly, the coating thicknesses varied between tens of microns and tens of millimeters. LFS PI coatings exhibited corrosion protection, and LFS PI + Cu showed improved antibacterial properties and provided sterilization against E-coli bacteria, which indicated high anti-fouling capacity.

**Fig. 13** Polarization curves for electrochemical corrosion testing in seawater and antibacterial testing for E-coli with a stainless steel 316 L plate, LFS PI and PI + Cu coatings. Modified from (Ref 32), reprinted with permission from Elsevier.

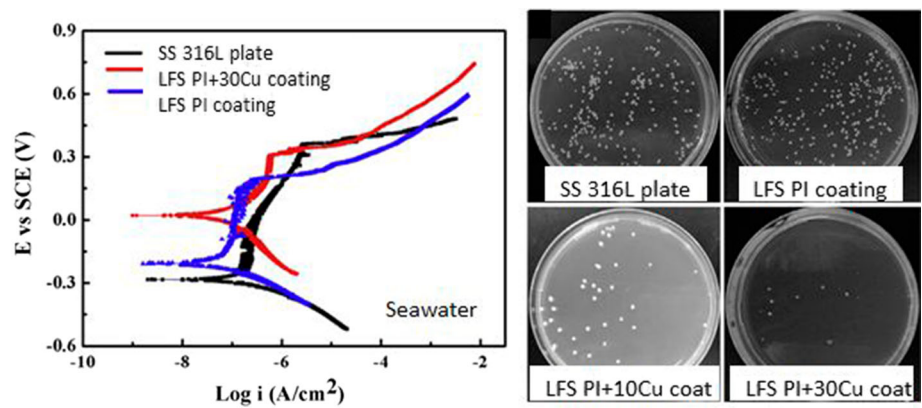


Figure 13 presents the corrosion behavior and the results for antibacterial testing with LFS PI and PI+Cu coatings as well as reference materials (Ref 32). Additionally, flame spraying of HDPE and HDPE+Cu powders was used to produce anti-fouling and corrosion-resistant coatings. In this study, Jia et al. (Ref 34) used particles that comprised a HDPE core with a Cu shell and flame sprayed them to produce HDPE + Cu composite coatings. The main goal of this enwrapped coating structure was to achieve controllable release of Cu for long-term anti-fouling performance (Ref 34).

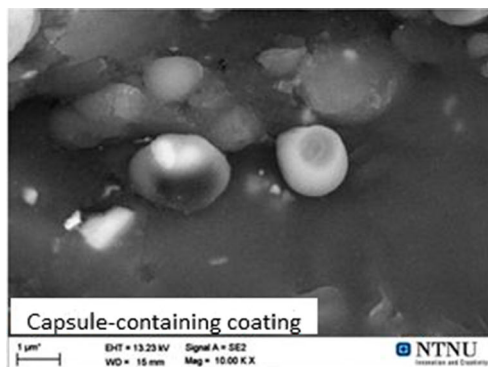
A novel approach to improve anti-fouling performance was presented by Liu et al. (Ref 27) who mixed HDPE with capsaicin and produced composite coatings by flame spraying. Dense coatings were manufactured, and they showed excellent anti-fouling properties due to the biocidal nature of naturally occurring capsaicin (Ref 27).

**Corrosion Protection**

Thermally sprayed fluoropolymer coatings have shown good corrosion resistance (Ref 12), and David et al. (Ref 40) studied FS MAH-g-LDPE coatings and observed improved corrosion resistance compared to FS LPDE

coatings. This was explained by higher coating adhesion and crystallinity seen with composite coatings. Modified (methacrylic acid, MA) PE coatings were produced by flame spraying to protect steel surfaces from corrosion. Delamination of the polymer coatings must be taken into account during studies of barrier layers, because if it occurs, corrosion protection fails (Ref 2).

The corrosion resistance of polymer coatings has been improved by blending polymers and nanoclays with flame-sprayed MAH-g-LDPE/UHMWPE coatings, as shown by Jeeva Jothi et al. (Ref 37). The corrosion rate in 3.5% NaCl was improved from 0.170 mm/year for bare mild steel to 0.028 mm/year for steel with FS MAH-g-LDPE/UHMWPE coatings (Ref 37). On the other hand, Taylor et al. (Ref 10) studied flame-sprayed PEEK coatings for corrosion protection with a mild steel substrate. They produced a dense coating, which showed an ~ 82% lower corrosion rate in 5% NaCl than the steel substrate. They also enhanced the wear resistance of the PEEK coating with annealing, which improved the mechanical properties of the coating. The semicrystalline PEEK coatings resulting after annealing had lower friction than coatings with amorphous structures (Ref 10). Furthermore, Lima et al. Ref 7 evaluated the corrosion and wear properties of FS



Coefficient of Friction (CoF) against AISI 316 steel ball rubbing

Coatings	Normal load, N	Average CoF	Length of the test, min
Capsules layer	5	0.16	10
	10	0.16	10
Nylon coating	5	0.47	30
	10	0.47	30
Capsule-containing coating (30% PAO capsules)	5	0.19	30
	10	0.17	30
Capsule-containing coating (50% PAO capsules)	5	0.14	30
	10	0.14	30
Capsule-containing coating (70% PAO capsules)	5	0.12	30
	10	0.14	30

**Fig. 14** Capsule-containing coating surfaces and coefficients of friction (CoF) for the FS capsule layer, Nylon coating and three capsule-containing coatings. Modified from (Ref 43), reprinted by permission from Springer Nature

PEEK, PEI and PA coatings and found that FS PA coatings had better resistance to abrasive wear. It was speculated that the better wear resistance was due to the higher crystallinity, better adhesion and lower residual stress. On the other hand, corrosion resistance was better for PA and PEEK coatings than for PEI coatings, which experienced color change and cracked during 2000-hour exposure in a H<sub>2</sub>SO<sub>4</sub> solution (Ref 7). In summary, thermally sprayed PEI, PA and PEEK coatings were viable solutions for corrosion and wear protection on metallic substrates (Ref 44).

### Self-lubrication

Lubrication of thermally sprayed polymer coatings was affected by using lubricant-filled polyurea microcapsules. Polyalphaolefin (PAO) and silicone oil were used as lubricants in the microcapsules (Ref 43). In this way, Armada et al. (Ref 43) produced liquid-solid self-lubricating coatings by using flame spraying. Process parameters were selected carefully to avoid destroying the microcapsules. Coatings were successfully produced, and self-healing behavior was observed, indicating improved friction properties (Fig. 14).

### Conclusions

Thermal spraying has been used to produce several different types of polymer-based coatings. Traditional flame spraying has been widely used to produce coatings offering corrosion and wear protection, as well as anti-icing and anti-fouling effects. Additionally, HVOF and plasma spraying have been used, but research has been focused more on cold spraying. Considerable research has improved the properties and performance of cold-sprayed polymer and polymer-composite coatings used to provide corrosion, wear and antibacterial protection. The latest developments with thermally and cold-sprayed polymer coatings have led to process optimization and feedstock tailoring, resulting in new application fields and high-performance solutions.

**Acknowledgments** The author would like to express her appreciation to Tampere University and the Tampere Institute for Advanced Study (Tampere-IAS) and the TS-SLIPS (Thermally Sprayed slippery liquid infused porous surfaces—toward durable anti-icing coatings) project funded by the Academy of Finland.

**Open Access** This article is licensed under a Creative Commons Attribution 4.0 International License, which permits use, sharing, adaptation, distribution and reproduction in any medium or format, as long as you give appropriate credit to the original author(s) and the source, provide a link to the Creative Commons licence, and indicate if changes were made. The images or other third party material in this

article are included in the article's Creative Commons licence, unless indicated otherwise in a credit line to the material. If material is not included in the article's Creative Commons licence and your intended use is not permitted by statutory regulation or exceeds the permitted use, you will need to obtain permission directly from the copyright holder. To view a copy of this licence, visit <http://creativecommons.org/licenses/by/4.0/>.

### References

1. E. Petrovicova and L.S. Schadler, Thermal Spraying of Polymers, *Int. Mater. Rev.*, 2002, **47**(4), p 169–190. <https://doi.org/10.1179/095066002225006566>
2. T. Sugama, R. Kawase, C.C. Berndt and H. Herman, An Evaluation of Methacrylic Acid-Modified Poly(Ethylene) Coatings Applied by Flame Spray Technology, *Prog. Org. Coat.*, 1995, **25**, p 205–216.
3. P. Vuoristo, E. Leivo, E. Turunen, M. Leino, P. Järvelä, and T. Mäntylä, in Evaluation of Thermally Sprayed and Other Polymeric Coatings for Use in Natural Gas Pipeline Components, Thermal Spray ed. C. Moreau, B. Marple Advancing the Science and Applying the Technology, ASM, Ohio, pp. 1693–1702 (2003)
4. L. Pawlowski, *The Science and Engineering of Thermal Spray Coatings*, John Wiley & Sons, New Jersey, 2008, p 647. (ISBN 978-0-471-49049-4)
5. H. Koivuluoto, E. Hartikainen and H. Niemelä-Anttonen, Thermally Sprayed Coatings: Novel Surface Engineering Strategy Towards Icephobic Solutions, *Materials*, 2020, **13**, p 1434. <https://doi.org/10.3390/ma13061434>
6. J.R.T. Branco and S.V. Campos, Wear Behavior of Thermally Sprayed PET, *Surf. Coat. Technol.*, 1999, **120–121**, p 476–481.
7. C.R.C. Lima, N.F.C. de Souza and F. Camargo, Study of Wear and Corrosion Performance of Thermal Sprayed Engineering Polymers, *Surf. Coat. Technol.*, 2013, **220**, p 140–143. <https://doi.org/10.1016/j.surfcoat.2012.05.051>
8. D. Lisjak, M. Begard, M. Bruehl, K. Bobzin, A. Hujanen, P. Lintunen, G. Bolelli, L. Lusvarghi, S. Ovtar and M. Drogenik, Hexaferrite/Polyester Composite Coatings for Electromagnetic-Wave Absorbers, *J. Therm. Spray Technol.*, 2011, **20**(3), p 638–644. <https://doi.org/10.1007/s11666-010-9607-8>
9. D. Niebuhr and M. Scholl, Synthesis and Performance of Plasma-Sprayed Polymer/Steel Coating System, *J. Therm. Spray Technol.*, 2005, **14**(4), p 487–494. <https://doi.org/10.1361/105996305X76496>
10. S. Tailor, N. Vashistha, A. Modi and S.C. Modi, One-Step Fabrication of Thermal Sprayed Polymer Coating on Metals, *Mater Res Express*, 2020, **7**, 016425. <https://doi.org/10.1088/2053-1591/ab6a4f>
11. G.W. Ehrenstein and S. Pongratz, *Resistance and Stability of Polymers*, Hanser Publications, Germany, 2013, p 1454. (ISBN 978-3-446-41645-1)
12. E. Leivo, T. Wilenius, T. Kinon, P. Vuoristo and T. Mäntylä, Properties of Thermally Sprayed Fluoropolymer PVDF, ECTFE, PFA and FEP Coatings, *Prog. Org. Coat.*, 2004, **49**, p 69–73.
13. W. Lock Sulen, K. Ravi, C. Bernard, Y. Ichikawa and K. Ogawa, Deposition Mechanism Analysis of Cold-Sprayed Fluoropolymer Coatings and Its Wettability Evaluation, *J. Therm. Spray Technol.*, 2020, **29**, p 1643–1659. <https://doi.org/10.1007/s11666-020-01059-w>
14. W. Xie, J. Wang and C.C. Berndt, Analysis of EMAA Splats on Glass and Mild Steel Substrates, *J. Therm. Spray Technol.*, 2014, **23**(3), p 317–324. <https://doi.org/10.1007/s11666-013-9989-5>

15. Z. Khalkhali, K.S. Rajan and J.P. Rothstein, Peening Effect of Glass Beads in the Cold Spray Deposition of Polymeric Powders, *J. Therm. Spray Technol.*, 2020, **29**, p 657–669. <https://doi.org/10.1007/s11666-020-01001-0>
16. S.P. Tambe, S.K. Singh, M. Patri and D. Kumar, Studies on Anticorrosive Properties of Thermally Sprayable EVA and EVAL Coating, *Prog. Org. Coat.*, 2010, **67**, p 239–245. <https://doi.org/10.1016/j.porgcoat.2009.12.002>
17. S.K. Singh, S.P. Tambe, V.S. Raja and D. Kumar, Thermally Sprayable Polyethylene Coatings for Marine Environment, *Prog. Org. Coat.*, 2007, **60**, p 186–193. <https://doi.org/10.1016/j.porgcoat.2007.07.028>
18. K. Ravi, T. Deplancke, K. Ogawa, J.-Y. Cavaille and O. Lame, Understanding Deposition Mechanism in cold Sprayed Ultra High Molecular Weight Polyethylene Coatings on metals by Isolated Particle Deposition Method, *Addit. Manuf.*, 2018, **21**, p 191–200. <https://doi.org/10.1016/j.addma.2018.02.022>
19. A. Rubin and P. Choi, *The Elements of Polymer Science and Engineering*, 3rd ed. Elsevier Inc, USA, 2013, p 561. (ISBN: 978-0-12-382178-2)
20. W. Xie, Thermal Spray Processing of Ethylene Methacrylic Acid and Polymer-Ceramic Composites. PhD Thesis, Swinburne University of Technology, p. 205 (2013)
21. V. Donadei, H. Koivuluoto, E. Sarlin and P. Vuoristo, Icephobic Behaviour and Thermal Stability of Flame-Sprayed Polyethylene Coating: The Effect of Process Parameters, *J. Therm. Spray Technol.*, 2020, **29**, p 241–254. <https://doi.org/10.1007/s11666-019-00947-0>
22. Z. Khalkhali and P. Rothstein, Characterization of the Cold Spray Deposition of a Wide Variety of Polymeric Powders, *Surf. Coat. Technol.*, 2020, **383**, p 125251. <https://doi.org/10.1016/j.surfcoat.2019.125251>
23. L.T. Duarte and E.M.J.R.T.V.F.C. Paula e SilvaBrancoLins, Production and Characterization of Thermally Sprayed Polyethylene Terephthalate Coatings, *Surf. Coat. Technol.*, 2004, **182**, p 261–267. <https://doi.org/10.1016/j.surfcoat.2003.08.062>
24. Y.S. Korobov, M.A. Belotserkovsky, K.M. Timofeev and S. Thomas, Adhesive Strength of Flame-Sprayed Polymer Coatings, Mechanics, Resource and Diagnostics of Materials and Structures (MRDMS-2016), *AIP Conf. Proc.*, 2016, **1785**, p 030011. <https://doi.org/10.1063/1.4967032>
25. G. Zhang, H. Liao, H. Yu, V. Ji, W. Huang, S.G. Mhaisalkar and C. Coddet, Correlation of Crystallization Behavior and Mechanical Properties of Thermal Sprayed PEEK Coating, *Surf. Coat. Technol.*, 2006, **200**, p 6690–6695. <https://doi.org/10.1016/j.surfcoat.2005.10.006>
26. K. Ravi, W. Lock Sulen, C. Bernard, Y. Ichikawa and K. Ogawa, Fabrication of Micro-/Nano-Structured Super-Hydrophobic Fluorinated Polymer Coatings by Cold-Spray, *Surf. Coat. Technol.*, 2019, **373**, p 17–24. <https://doi.org/10.1016/j.surfcoat.2019.05.078>
27. Y. Liu, X. Shao, J. Huang and H. Li, Flame Sprayed Environmentally Friendly High Density Polyethylene (HDPE)–capsaicin Composite Coatings for Marine Antifouling Applications, *Mater. Lett.*, 2019, **238**, p 46–50. <https://doi.org/10.1016/j.matlet.2018.11.144>
28. H. Koivuluoto, C. Stenroos, M. Kylmälahti, M. Apostol, J. Kii-lakoski and P. Vuoristo, Anti-icing Behavior of Thermally Sprayed Polymer Coatings, *J. Therm. Spray Technol.*, 2017, **26**, p 150–160. <https://doi.org/10.1007/s11666-016-0501-x>
29. H. Niemelä-Anttonen, H. Koivuluoto, M. Kylmälahti, J. Laakso, P. Vuoristo, in Thermally Sprayed Slippery and Icephobic Surfaces, Proceedings of International Thermal Spray Conference, ITSC2018, ed. by F. Azarmi, K. Balani, T. Eden, T. Hussain, Y.-C. Lau, H. Li, K. Shinoda (eds.), 7–10 May, Orlando, Florida, USA, pp. 380–384
30. A. Soveja, S. Costil, H. Liao, P. Sallamand and C. Coddet, Remelting of Flame Spraying PEEK Coating Using Lasers, *J. Therm. Spray Technol.*, 2010, **19**(1–2), p 439–447. <https://doi.org/10.1007/s11666-009-9421-3>
31. K. Alamara, S.S. Samandari and C.C. Berndt, Splat Formation of Polypropylene Flame Sprayed onto a Flat Surface, *Surf. Coat. Technol.*, 2010, **205**, p 2518–2524. <https://doi.org/10.1016/j.surfcoat.2010.09.056>
32. X. Wang, Y. Liu, Y. Gong, X. Suo and H. Li, Liquid Flame Spray Fabrication of Polyimide-Copper Coatings for Antifouling Applications, *Mater. Lett.*, 2017, **190**, p 217–220. <https://doi.org/10.1016/j.matlet.2017.01.028>
33. Y. Liu, X. Xu, X. Suo, Y. Gong and H. Li, Suspension Flame Spray Construction of Polyimide-Copper Layers for Marine Antifouling Applications, *J. Therm. Spray Technol.*, 2018, **27**, p 98–105. <https://doi.org/10.1007/s11666-017-0653-3>
34. Z. Jia, Y. Liu, Y. Wang, Y. Gong, P. Jin, X. Suo and H. Li, Flame spray Fabrication of Polyethylene-Cu composite coatings with Enwrapped Structures: A New Route for Constructing Antifouling Layers, *Surf. Coat. Technol.*, 2017, **309**, p 872–879. <https://doi.org/10.1016/j.surfcoat.2016.10.071>
35. Z. Jia, J. Huang, Y. Gong, P. Jin, X. Suo and H. Li, Incorporation of Copper Enhances the Anti-Ageing Property of Flame-Sprayed High-Density Polyethylene Coatings, *J. Therm. Spray Technol.*, 2017, **26**, p 409–416. <https://doi.org/10.1007/s11666-017-0525-x>
36. A. Chebbi and J. Stokes, Thermal Spraying of Bioactive Polymer Coatings for Orthopaedic Applications, *J. Therm. Spray Technol.*, 2012, **21**(3–4), p 719–730. <https://doi.org/10.1007/s11666-012-9764-z>
37. K. JeevaJothi, A.U. Santhoskumar, S. Amanulla and K. Palani-velu, Thermally Sprayable Anti-corrosion Marine Coatings Based on MAH-g-LDPE/UHMWPE Nanocomposites, *J. Therm. Spray Technol.*, 2014, **23**(8), p 1413–1424. <https://doi.org/10.1007/s11666-014-0153-7>
38. Y. Li, Z. Man, X. Lin, L. Wei, H. Wang and M. Lei, Role of Well-Dispersed Carbon Nanotubes and Limited Matrix Degradation on Tribological Properties of Flame-Sprayed PEEK Nanocomposite Coatings, *J. Tribol.*, 2022, **144**, p 012101.
39. D.E. Crawmer, Thermal Spray Processes, *Handbook of Thermal Spray Technology*. J.R. Davis Ed., ASM International, USA, 2004, p 54–76
40. R. David, S.P. Tambe, S.K. Singh, V.S. Raja and D. Kumar, Thermally Sprayable Grafted LDPE/Nanoclay Composite Coating for Corrosion Protection, *Surf. Coat. Technol.*, 2011, **205**, p 5470–5477. <https://doi.org/10.1016/j.surfcoat.2011.06.022>
41. K. Alamara, S. Saber-Samandari and C.C. Berndt, Splat Taxonomy of Polymeric Thermal Spray Coating, *Surf. Coat. Technol.*, 2011, **205**, p 5028–5034. <https://doi.org/10.1016/j.surfcoat.2011.05.002>
42. Y. Bao, D.T. Gawne and T. Zhang, Cure Kinetics of Flame-Sprayed Thermoset Coatings, *Surf. Coat. Technol.*, 2012, **207**, p 89–95. <https://doi.org/10.1016/j.surfcoat.2012.06.007>
43. S. Armada, R. Schmid, S. Equey, I. Fagoaga and N. Espallargas, Liquid-Solid Self-Lubricated Coatings, *J. Therm. Spray Technol.*, 2013, **22**(1), p 10–17. <https://doi.org/10.1007/s11666-012-9847-x>
44. C.R.C. Lima, M.A.R. Mojena, C.A.D. Rovere, N.F.C. de Souza and H.D.C. Fals, Slurry Erosion and Corrosion Behavior of Some Engineering Polymers Applied by Low-Pressure Flame Spray, *J. Mater. Eng. Perform.*, 2016, **25**(11), p 4911–4918. <https://doi.org/10.1007/s11665-016-2317-8>
45. V. Donadei, H. Koivuluoto, E. Sarlin and P. Vuoristo, Lubricated Icephobic Coatings Prepared by Flame Spraying with Hybrid Feedstock Injection, *Surf. Coat. Technol.*, 2020, **403**, p 126396. <https://doi.org/10.1016/j.surfcoat.2020.126396>
46. V. Donadei, H. Koivuluoto, E. Sarlin, H. Niemelä-Anttonen, T. Varis and P. Vuoristo, The Effect of Mechanical and Thermal Stresses on the Performance of Lubricated Icephobic Coatings

- During Cyclic Icing/Deicing Tests, *Prog. Org. Coat.*, 2021 <https://doi.org/10.1016/j.porgcoat.2021.106614>
47. L. Jackson, M. Ivosevic, R. Knight and R.A. Cairncross, Sliding Wear Properties of HVOF Thermally Sprayed Nylon-11 and Nylon-11/Ceramic Composites on Steel, *J. Therm. Spray Technol.*, 2007, **16**(5–6), p 927–932. <https://doi.org/10.1007/s11666-007-9088-6>
  48. K. Patel, C.S. Doyle, D. Yonekura and B.J. James, Effect of Surface Roughness Parameters on Thermally Sprayed PEEK Coatings, *Surf. Coat. Technol.*, 2010, **204**, p 3567–3572. <https://doi.org/10.1016/j.surfcoat.2010.04.026>
  49. B.P. Withy, M.M. Hyland and B.J. James, The Effect of Surface Chemistry and Morphology on the Properties of HVAF PEEK Single Splats, *J. Therm. Spray Technol.*, 2008, **17**(5–6), p 631–636. <https://doi.org/10.1007/s11666-008-9250-9>
  50. L.S. Schadler, K.O. Laul, R.W. Smith and E. Petrovicova, Microstructure and Mechanical Properties of Thermally Sprayed Silica/Nylon Nanocomposites, *J. Therm. Spray Technol.*, 1997, **6**(4), p 475–485.
  51. A. Stravato, R. Knight, V. Mochalin and S.C. Picardi, HVOF-Sprayed Nylon-11 + Nanodiamond Composite Coatings: Production & Characterization, *J. Therm. Spray Technol.*, 2008, **17**(5–6), p 812–817. <https://doi.org/10.1007/s11666-008-9253-6>
  52. T. Zhang, D.T. Gawne and Y. Bao, The influence of Process Parameters on The Degradation of Thermally Sprayed Polymer Coatings, *Surf. Coat. Technol.*, 1997, **96**, p 337–344.
  53. C. Mateus, S. Costil, R. Bolot and C. Coddet, Ceramic/Fluoropolymer Composite Coatings by Thermal spraying—a Modification of Surface Properties, *Surf. Coat. Technol.*, 2005, **191**, p 108–118. <https://doi.org/10.1016/j.surfcoat.2004.04.084>
  54. S. Costil, C. Mateus and C. Coddet, Ceramic/Fluoropolymer Composite Coatings by Plasma Spraying, *Surf. Coat. Technol.*, 2006, **201**, p 2020–2027. <https://doi.org/10.1016/j.surfcoat.2006.04.051>
  55. J. Wu, P.R. Munroe, B. Withy and M.M. Hyland, Study of the Splat-Substrate Interface for a PEEK Coating Plasma-Sprayed onto Aluminum Substrates, *J. Therm. Spray Technol.*, 2010, **19**(1–2), p 42–48. <https://doi.org/10.1007/s11666-009-9430-2>
  56. N. Sanpo, M.L. Tan, P. Cheang and K.A. Khor, Antibacterial Property of Cold-Sprayed HA-Ag/PEEK Coating, *J. Therm. Spray Technol.*, 2009, **18**(1), p 10–15. <https://doi.org/10.1007/s11666-008-9283-0>
  57. N. Sanpo, S.M. Ang, P. Cheang and K.A. Khor, Antibacterial Property of Cold Sprayed Chitosan-Cu/Al Coating, *J. Therm. Spray Technol.*, 2009, **18**(4), p 600–608. <https://doi.org/10.1007/s11666-009-9391-5>
  58. A.S. Alhulaifi, G.A. Buck and W.J. Arbegast, Numerical and Experimental Investigation of Cold Spray Gas Dynamic Effects for Polymer Coating, *J. Therm. Spray Technol.*, 2012, **21**(5), p 852–862. <https://doi.org/10.1007/s11666-012-9743-4>
  59. K. Ravi, Y. Ichikawa, T. Deplancke, K. Ogawa, O. Lame and J.Y. Cavaille, Development of Ultra-High Molecular Weight Polyethylene (UHMWPE) Coating by Cold Spray Technique, *J. Therm. Spray Technol.*, 2015, **24**(6), p 1015–1025. <https://doi.org/10.1007/s11666-015-0276-5>
  60. N. Ata, N. Ohtake and H. Akasaka, Polyethylene-Carbon Nanotube Composite Film Deposited by Cold Spray Technique, *J. Therm. Spray Technol.*, 2017, **26**, p 1541–1547. <https://doi.org/10.1007/s11666-017-0617-7>
  61. T.B. Bush, Z. Khalkhali, V. Champagne, D.P. Schmidt and J.P. Rothstein, Optimization of Cold Spray Deposition of High-Density Polyethylene Powders, *J. Therm. Spray Technol.*, 2017, **26**, p 1548–1564. <https://doi.org/10.1007/s11666-017-0627-5>
  62. C.A. Bernard, H. Takana, G. Diguët, K. Ravi, O. Lame, K. Ogawa and J.-Y. Cavaille, Thermal gradient of in-flight polymer particles during cold spraying, *J. Mater. Process. Tech.*, 2020, **286**, p 116805. <https://doi.org/10.1016/j.jmatprotec.2020.116805>
  63. N.K. Singh, K.Z. Uddin, J. Muthulingam, R. Jha and B. Koohbor, Analyzing the Effects of Particle Diameter in Cold Spraying of Thermoplastic Polymers, *J. Therm. Spray Technol.*, 2021, **30**, p 1226–1238. <https://doi.org/10.1007/s11666-021-01219-6>
  64. Z. Khalkhali, W. Xie, V.K. Champagne, J.-H. Lee and J.P. Rothstein, A comparison of Cold Spray Technique to Single Particle Micro-Ballistic Impacts for the Deposition of Polymer Particles on Polymer Substrates, *Surf. Coat. Technol.*, 2018, **351**, p 99–107. <https://doi.org/10.1016/j.surfcoat.2018.07.053>
  65. K. Ravi, Y. Ichikawa, K. Ogawa, T. Deplancke, O. Lame and J.-Y. Cavaille, Mechanistic Study and Characterization of Cold-Sprayed Ultra-High Molecular Weight Polyethylene-Nano-Ceramic Composite Coating, *J. Therm. Spray Technol.*, 2016, **25**(1–2), p 160–169. <https://doi.org/10.1007/s11666-015-0332-1>

**Publisher's Note** Springer Nature remains neutral with regard to jurisdictional claims in published maps and institutional affiliations.